Atmos. Chem. Phys. Discuss., 13, 29811–29843, 2013
www.atmos-chem-phys-discuss.net/13/29811/2013/
doi:10.5194/acpd-13-29811-2013

Atmospheric Chemistry and Physics
Discussions
Open Access

Synthesis and coherent vibrational laser spectroscopy of putative molecular constituents in isoprene-derived secondary organic aerosol particles

C. J. Ebben[1,*], B. F. Strick[1,*], M. A. Upshur[1], H. M. Chase[1], J. L. Achtyl[1], R. J. Thomson[1], and F. M. Geiger[1]

[1]Department of Chemistry, Northwestern University, Evanston, IL 60208, USA
[*]These authors contributed equally to this work.

Received: 17 October 2013 – Accepted: 22 October 2013 – Published: 13 November 2013

Correspondence to: R. J. Thomson (r-thomson@northwestern.edu) and
F. M. Geiger (geigerf@chem.northwestern.edu)

Published by Copernicus Publications on behalf of the European Geosciences Union.

Abstract

SOA particle formation ranks among the least understood processes in the atmosphere, rooted in part in (a) the limited knowledge about SOA chemical composition; (b) the availability of only little concrete evidence for chemical structures; and (c) little availability of reference compounds needed for benchmarking and chemical identification in pure and homogenous form. Here, we address these challenges by synthesizing and subjecting to physical and chemical analysis putative isoprene-derived SOA particle constituents. Our surface-selective spectroscopic analysis of these compounds is followed by comparison to synthetic SOA particles prepared at the Harvard Environmental Chamber (HEC) and to authentic SOA particles collected in a tropical forest environment, namely the Amazon Basin, where isoprene oxidation by OH radicals has been reported to dominate SOA particle formation (Martin et al., 2010b; Sun et al., 2003; Hudson et al., 2008; Yasmeen et al., 2010). We focus on the epoxides and tetraols that have been proposed to be present in the SOA particles. We characterize the compounds prepared here by a variety of physical measurements and polarization-resolved vibrational sum frequency generation (SFG), paying particular attention to the phase state (condensed vs. vapor) of four epoxides and two tetraols in contact with a fused silica window. We compare the spectral responses from the tetraol and epoxide model compounds with those obtained from the natural and synthetic SOA particle samples that were collected on filter substrates and pressed against a fused silica window and discuss a possible match for the SFG response of one of the epoxides with that of the synthetic SOA particle material. We conclude our work by discussing how the approach described here will allow for the study of the SOA particle formation pathways from first- and second-generation oxidation products by effectively “fast-forwarding” through the initial reaction steps of particle nucleation via a chemically resolved approach aimed at testing the underlying chemical mechanisms of SOA particle formation.

1 Introduction

Secondary organic aerosol (SOA) particles are important in the climate system as they can lead to significant negative radiative forcing, especially over the world's large forest ecosystems (Kanakidou et al., 2005; Murray et al., 2000; Williams et al., 2011). Despite this prominent role, SOA particle formation ranks among the least understood processes in the atmosphere (Kanakidou et al., 2005; Hallquist et al., 2009; Goldstein and Galbally, 2007; Galbally et al., 2007; Weiss et al., 2008a), rooted in part in the limited knowledge about SOA chemical composition. Molecular studies (Yasmeen et al., 2010; Weiss et al., 2008b; Kleiber et al., 2009; Wang et al., 2005b; Gao et al., 2010; Mena-Carrasco et al., 2009; Huynh et al., 2003; Palaniappan et al., 2009; Greenham et al., 1996; Sharma et al., 2003; Tolocka et al., 2004; Grassian, 2009; Docherty et al., 2005; Heaton et al., 2009) aimed at bridging this knowledge gap support the hypothesis that the products formed from the gas phase oxidization of biogenic volatile organic compounds react with one another to form species with lower and lower vapor pressures, ultimately leading to SOA particle formation. Heterogeneous processes such as physisorption and surface reactions are important for conditions of condensational particle growth. The formation of larger particles through coagulative growth may also be largely influenced by processes occurring at the surfaces of the particles, especially under conditions of low relative humidity for which SOA particle material has been shown to be solid.

One key challenge in understanding SOA particle growth which is addressed in this present work is that little concrete evidence for chemical structures is available. Moreover, most reference compounds needed for benchmarking and chemical identification in, for instance, mass spectrometric studies of SOA particles (Heaton et al., 2007, 2009), are not available in pure and homogenous form from commercial sources. A third challenge is that laboratory model studies typically begin with hydrocarbon precursors, such as isoprene or α-pinene, to form SOA particles, while field studies sample SOA particles at various stages along their formation pathway, which is currently unknown. Finally, few molecularly specific techniques exist that are appropriate for probing the particle/gas interface or the surfaces of samples of putative SOA particle constituents directly.

Here, we address these challenges by synthesizing and subjecting to physical and chemical analysis putative isoprene-derived SOA particle constituents. Our surface-selective spectroscopic analysis of these compounds is followed by comparison to synthetic SOA particles prepared at the Harvard Environmental Chamber (HEC) and to authentic SOA particles collected in a tropical forest environment, namely the Amazon Basin (Martin et al., 2010a), where isoprene oxidation by OH radicals has been reported to dominate SOA particle formation (Martin et al., 2010b; Sun et al., 2003; Hudson et al., 2008; Yasmeen et al., 2010). As part of this work, we focus on the epoxides (Sun et al., 2003) and tetraols (Yasmeen et al., 2010) that have been proposed to be present in the SOA particles and that are characterized by oxygen-to-carbon (O/C) ratios (Lewis et al., 2005) that fall into the 0.4+/-0.1 range typical for SOA particles in tropical forests (Nelson and Chandler, 2004). Following a brief description of the synthesis and the analytical methods, we characterize the compounds prepared here by a variety of physical measurements and surface-selective spectroscopic probes. We collect polarization-resolved vibrational sum frequency generation (SFG) spectra of condensed phase and vapor phase samples of four epoxides and two tetraols in contact with a fused silica window. We compare the spectral responses from the tetraol and epoxide model compounds with those obtained from the natural and synthetic SOA particle samples that were collected on filter substrates and pressed against a fused silica window and discuss a possible match for the SFG response of one of the epoxides with that of the synthetic SOA particle material. We conclude our work by discussing how the approach described here will allow for the study of the SOA particle formation pathways from first- and second-generation oxidation products by effectively "fast-forwarding" through the initial reaction steps of particle nucleation via a chemically resolved approach aimed at testing the underlying chemical mechanisms of SOA particle formation.

2 Experimental

2.1 Synthesis of putative isoprene-derived SOA particle precursors

During the isolation and structural determination of naturally occurring molecules, concrete evidence for tentative structural assignments is often obtained by synthesizing the proposed structures in the laboratory. This need for de novo synthesis of putative structures is especially important when the compounds in question exist naturally in such small quantities that isolation of enough material for thorough spectroscopic analysis is not practical or even possible. In this respect, the numerous organic molecules formed in the atmosphere from naturally occurring isoprene represent a challenge due to difficulties associated with their collection in meaningful amounts (µg- or mg-amounts for offline analytical studies) and the complexity of the thus obtained mixtures. In order to perform physical studies on these putative species that are relevant to atmospheric processes, we sought to obtain a suite of pure chemical standards. To this end, we have accomplished the synthesis of six putative hydroxyl radical-mediated, isoprene-derived oxidation products (Fig. 1).

Epoxides 1–4 were synthesized in an analogous fashion to the procedures reported by Surratt and coworkers (Zhang et al., 2012). While all samples reported herein are racemic, efforts were made to prepare diastereomerically pure samples where possible.

The internal epoxides 1 and 2 were prepared in diastereomerically pure form starting from 3-methyl-2-buten-1-ol and 3-methyl furan-2(5*H*)-one, respectively. The terminal epoxides 3 and 4 were synthesized as 1 : 1 mixtures of inseparable diastereomers starting from 2-methyl-2-vinyloxirane. Tetraols 5 and 6 were prepared in diastereomerically pure form starting from protected *trans* and *cis* 2-methylbut-2-ene-1,4-diols, respectively (Zhang et al., 2012; Fontana et al., 2000). The procedures employed in these syntheses are described in further detail in the Supplement.

2.2 Synthetic and field-collected SOA particle material derived from isoprene

We compare the SFG spectra obtained from the epoxides and tetraols prepared here to those obtained from aerosol particles synthesized as a model system from the photochemical reaction of isoprene and OH radicals at the Harvard Environmental Chamber (HEC), (Ebben et al., 2011b; Chen et al., 2011) as well as from submicron-sized SOA particles collected in the central Amazon Basin during the AMAZE-08 campaign (Martin et al., 2010a), chosen as an example of a tropical forest whose air is typically rich in isoprene. We thus expect the SFG spectra obtained from the surfaces of the synthetic and field-derived particles to be due to products of isoprene oxidation pathways. The approach for our analysis of SOA particle material prepared at the HEC and collected at the AMAZE-08 field site by SFG has been described in detail in our prior work (Ebben et al., 2012).

2.3 Vibrational sum frequency generation

The surface-specific probe employed here is based on a SFG setup that has been previously described (Buchbinder et al., 2009; Voges and Geiger, 2005; Voges et al., 2007; Stokes et al., 2009a, c). Briefly, we utilize a Ti:S femtosecond laser system operating at 1 kHz repetition rate (Spectra Physics, Spitfire Pro). Half of the 800 nm output is used to pump an optical parametric amplifier (Spectra Physics, OPA 800C) for generating tunable broadband (full width at half max of $\sim 150\,\mathrm{cm^{-1}}$) infrared light appropriate for covering the aromatic and aliphatic C–H stretching regions. At the sample surface, the IR light field is upconverted using a visible pump beam filtered with a narrow bandpass filter yielding an 800 nm pump pulse with a bandwidth of 1.57 nm. To avoid optical damage, the incident pulse energies and foci are limited to 2 µJ and 50 µm in diameter, respectively. Internal reflection geometry, in which the incident light fields pass through the fused silica window to reach the sample interface, is utilized in all experiments. The ssp polarization combination that is employed in these experiments probes those components of the vibrational transition dipole moments that are oriented perpendicular to the solid substrate. SFG experiments are repeated several times from at least two different sample spots for spin-coated samples, or from vapor samples prepared separately. Spectra shown in this work are averages of the individual spectra. The Supplement shows the individual spectra for the various compounds under investigation in this work. In general, we find that the frequency positions of the spectral features vary by less than 8 cm^{-1} among the individual spectra. The full C–H stretching frequency region is analyzed with a hybrid scanning/broadband method pioneered by Walker and coworkers (Esenturk and Walker, 2004). Spectra are collected for 7 acquisitions lasting 2 min each, in order to increase signal-to-noise. SFG spectra are referenced to the SFG response from a gold substrate to account for the energy distribution in the incident IR pulse, and the frequencies are calibrated using a polystyrene standard (ICL Crystal Laboratories).

2.4 Sample configurations

The synthetic epoxide and tetraol samples were analyzed at room temperature by SFG by contacting a fused silica window with (a) their equilibrium vapor pressure (Handbook of Chemistry and Physics, 1997) and (b) their condensed phase following spin-coating of the sample dissolved in deuterated methanol. Synthetic SOA particle material, condensed over the course of several days onto 50 nm-sized ammonium sulfate seed particles during the reaction of isoprene and OH radicals at the HEC and subsequently collected on Teflon filters as described in our earlier work, (Ebben et al., 2011b) was probed by SFG by pressing a fused silica window against a Teflon filter containing SOA particle material (Ebben et al., 2011a, 2012). Finally, field-derived SOA particle material, collected on nucleopore impactor substrates sampled using a micro-orifice uniform-deposit impactor (MOUDI) (Marple et al., 1991) in the central Amazon Basin from 9 April 2008 to 17 April 2008 at the site of the AMAZE-08 campaign (Martin et al., 2010a), was probed by SFG in the same way as the synthetic SOA particle material prepared at the HEC. Before collecting an SFG spectrum, all fused silica substrates were rinsed and sonicated in methanol and Millipore water, nitrogen and oven dried,

and plasma cleaned prior to exposure to samples. Substrates not exposed to sample compounds showed no evidence of C–H stretches.

In the window/vapor experiments of the epoxides, a volume of approximately 30 µL of sample was injected through a syringe into the void space of a custom-built Teflon sample cell having an opening against which a fused silica window was sealed using an O-ring. Vapor experiments with the gel-like tetraol samples were carried out by spreading a gel drop of the sample at the bottom of a fused silica window. Following the introduction of the sample to the sample cell and window, the vapor of the condensed phase samples was allowed to equilibrate in the void space of the cell. In this configuration, the incident laser fields did not illuminate the condensed phase sample.

In addition to window/vapor experiments, all of the compounds were dissolved to 100 mM in deuterated methanol and then spin-coated directly onto fused silica windows, which were then placed against the sample cell with an O-ring. In this configuration, the incident laser fields did illuminate the spin-coated film.

3 Results and discussion

3.1 Phase states

There exists a keen interest in determining the phase state of SOA particles (Nelson et al., 2001; Huang et al., 2008), as reactive processing inside the particle bulk may be turned off upon particle solidification and may compete with surface reactions if the particles are not solid. Given this interest, and given the sensitivity of SFG spectroscopy to interfaces between materials undergoing phase changes, (Miranda and Shen, 1999; Wei et al., 2002) we report here which of the model compounds are liquid vs. solid at temperatures relevant to the upper and lower troposphere. In the following section, we also discuss differences in the vibrational SFG responses obtained from vapor phase vs. condensed phase model compounds in contact with the fused silica windows employed here.

We find that each of the epoxides is a liquid at room temperature, becoming increasingly viscous (but not solid) with lower and lower temperatures down to −40 °C. The two tetraol compounds described in this work are also not solid at room temperature. However, in contrast to the epoxides that form them, they are gel-like down to −40 °C. The gel state made it difficult to handle the tetraols with a syringe. As described in the prior section, the vapor experiments with the tetraol samples were therefore carried out by spreading a gel drop of the sample at the bottom of a fused silica window, followed by equilibration of the vapor in the space between the window and the cell. Room-temperature vapor pressures over the epoxides and tetraols – and their binding constants for interaction with the solid fused silica substrate – are evidently high enough to produce the sizable SFG responses at the vapor/solid interface reported here.

3.2 Vibrational sum frequency generation spectra

Figures 2a, b and 3a, b summarize our findings from carrying out ssp-polarized vibrational SFG spectroscopic analyses of the epoxides and tetraols in the two phase states studied here (vapor and condensed phase), of isoprene-derived synthetic SOA particle material, and of field-derived SOA particles in the 1.0 µm size fraction. The latter was chosen as a representative spectrum of PM_1-sized (i.e. below 1 µm in diameter) SOA particles collected during AMAZE-08 (Ebben et al., 2012). Using our sample storage procedures, SFG spectra of the isoprene-derived synthetic SOA particle material do not change over the duration of three years, as shown in the Supplement. The following two sections discuss the results obtained from the epoxides and the tetraols, and the last section compares the results to those obtained from the synthetic and field-derived SOA particles samples.

3.2.1 Epoxides

Figure 2a shows that a peak at 2955 cm^{-1} dominates the SFG spectra of fused silica windows in contact with the vapor-phase epoxides. The spectra also exhibit smaller signal contributions around 2880 cm^{-1}. SFG responses from methyl groups of long-chain hydrocarbons usually occur at 2960 cm^{-1} and 2940 cm^{-1}, attributable to the Fermi resonance of the CH_3 asymmetric stretch with a CH_3 bending overtone and the CH_3 asymmetric stretch, (Miranda and Shen, 1999; Chen et al., 2002; Opdahl et al., 2002) and at 2880 cm^{-1}, which is attributable to the CH_3 symmetric stretch (Miranda and Shen, 1999; Conboy et al., 1997, 1998). These SFG responses are typically the dominant and most intense features in the SFG spectra of hydrocarbons. We therefore attribute the strong peak near 2955 cm^{-1} to the asymmetric methyl stretch and/or its Fermi resonance and the smaller peak near 2880 cm^{-1} to the symmetric methyl stretch. However, the molecules studied here also contain one or two hydroxyl-substituted methylene groups. SFG spectra of analogous ethanolic methylene groups within a series of alcohols have been reported in one study by Wang and co-workers to exhibit a symmetric stretch at 2886 cm^{-1} and a Fermi resonance at 2974 cm^{-1} (Lu et al., 2004), located where the SFG spectra of the epoxides studied here also show some intensity. Epoxides 3 and 4 also contain a vicinal diol moiety having one methylene group. The SFG responses from this methylene group may be compared to those reported by the Wang group for the two methylene groups at the glycol/vapor interface (Lu et al., 2004), for which symmetric and asymmetric stretches occur at 2870 cm^{-1} with strong intensity and at 2900 cm^{-1} with quite low intensity, respectively, along with a Fermi resonance having medium signal intensity at 2938 cm^{-1}. The SFG spectra reported here exhibit SFG signal intensity at these frequencies, but the contributions are either not well resolved spectroscopically or overlap with the strong SFG responses produced by the methyl group.

The SFG spectra of epoxides 3 and 4 show some intensity between 3050 cm^{-1} and 3020 cm^{-1}. In SFG spectroscopy, this frequency region is typically associated with aromatic C–H groups, (Hommel and Allen, 2003; Weiss et al., 2007) or vinylic groups (Buchbinder et al., 2009; Stokes et al., 2008a, 2009a, b), which are not present in these two species. While the SFG responses observed from epoxides 3 and 4 between 3050 cm^{-1} and 3020 cm^{-1} are weak, they are likely to indicate the presence of the single methylene group attached to the strained epoxide ring structure in these compounds: previous SFG studies have shown that as the number of carbon atoms in a cyclic hydrocarbon decreases, and the C–C single bonds become increasingly strained, the vibrational frequencies of the methylene symmetric stretches shift beyond 3000 cm^{-1} (Watson, 2010). Furthermore, the IR spectra of bromocyclopropane, (Diallo and Waters, 1988) cyclopropane-d_1, (Diallo and Waters, 1988) cyclopropane-1,1-d_2, (Keeports and Eggers, 1984) cyclopropane 1,1,2,2-d_4, (Keeports and Eggers, 1984) and cyclopropane (Diallo and Waters, 1988; Spiekermann et al., 1980) all show vibrational responses beyond 3000 cm^{-1}. Based on these literature reports, we assign the peak at ~ 3020 cm^{-1} that is exhibited by epoxides 3 and 4 to the symmetric stretching mode of the single methylene group in the epoxide motif of these molecules.

Finally, the epoxides studied here all contain one methine group, which is generally observed by SFG at a frequency of approximately 2900 cm^{-1} (Buck and Himmelhaus, 2001; Lu et al., 2005). The SFG spectra shown in Fig. 2a and b exhibit little intensity at those frequencies, indicating that the contributions from the methine group in the epoxides is quite weak.

From our spectral analysis, we conclude that the epoxides studied here produce SFG signals that are mainly due to their CH_3 asymmetric stretch and/or Fermi resonance, with minor contributions from the CH_3 symmetric stretch and some contribution from the methylene groups, depending on whether the epoxide ring is internally or terminally located.

As described in the experimental section, the SFG experiments were also carried out by spin coating the same IEPOX samples in deuterated methanol onto fused silica windows. Figure 2b shows increased SFG signal intensity in the symmetric stretching region (i.e. below 2900 cm^{-1}) for all compounds analyzed when compared to Fig. 2a.

Generally, the ratio of the SFG signal intensities from the symmetric and the asymmetric stretching modes of a methyl group informs on that group's molecular tilt angle (Yang et al., 2002). The increased SFG signal intensity obtained from the methyl symmetric stretching mode suggests that the C_{3v} symmetry axes of the methyl groups of the four epoxides studied here are tilted much more towards the surface normal for the spin-coated samples than for the vapor phase samples. The ratio of the SFG signal intensities from the symmetric and the asymmetric stretching modes may thus be used as a marker for distinguishing vapor samples from condensed phase samples in contact with the fused silica windows. Finally, the contributions from the strained methylene group in epoxides 3 and 4 that we observed above 3000 cm^{-1} in the window/vapor experiments are much weaker, if present at all, in the condensed phase samples. Moreover, well-resolved spectral features at the frequencies associated with ethanolic or glycolic methylene groups are not observed in Fig. 2b. Taken together, our findings indicate significant restructuring of the epoxides at the fused silica windows employed here depending on whether they are in the condensed or vapor phase.

3.2.2 Tetraols

As mentioned in the introduction, ongoing reactions with hydroxyl radicals under acidic low NO_x conditions can lead to the formation of 2-methyltetraols from IEPOX precursors, which may be part of SOA particle material. We therefore analyzed two tetraols, 5 and 6, which are *syn*- and *anti*-diastereomers of one another. Just like in the case of the epoxides, we carried out our analysis for vapor and spin-coated tetraol compounds in contact with fused silica windows (Fig. 3a and b).

As expected, neither tetraol shows appreciable SFG signal intensity at frequencies exceeding 3000 cm^{-1}, which is consistent with the absence of aromatic, vinylic, or strained methylene groups in these tetraols. Similar to the epoxides, the SFG spectra of tetraols 5 and 6 vapor display a dominant feature at 2946 and 2953 cm^{-1}, respectively, which we attribute to the methyl asymmetric stretch and/or Fermi resonance of the methyl group in the tetraols for the reasons outlined above. As in the case of the epoxides, the methyl symmetric stretching contribution to the SFG spectra increases – quite substantially in fact – when the samples are spin-coated as opposed to present in the vapor phase. Furthermore, while *syn*-2-methyltetraol (5) features only one peak in this region at 2880 cm^{-1}, *anti*-2-methyltetraol (6) shows an additional fairly well resolved contribution at 2840 cm^{-1}, which we attribute here to contributions from the symmetric methylene C-H stretches for the reasons outlined above. Just like the epoxides, the two tetraols studied here contain one methine group. Unlike for the epoxides, however, the SFG spectra of the tetraols in contact with the fused silica windows (except for the tetraol 6 vapor) exhibit significant SFG signal intensity at 2900 cm^{-1}, which is where methine stretches have been reported to occur (Buck and Himmelhaus, 2001; Lu et al., 2005). Finally, we find that the SFG spectra obtained from the fused silica surface in contact with the room temperature equilibrium vapor pressure above a drop of tetraol 5 are about two to three times higher in intensity than those obtained from tetraol 6. This finding could be due to a less ordered interfacial structure in terms of the methyl and methylene oscillators, or due to a lower vapor pressure of the *syn*- (5) vs. the *anti*-tetraol (6).

3.2.3 Comparison to synthetic and field-derived SOA particle material

In this section, we compare the SFG spectra obtained from epoxides (1–4) and tetraols (5 and 6) to those obtained from synthetic and field-derived SOA particle material. We report and discuss a possible match in the SFG spectra obtained from one of the model compounds and the synthetic SOA particle samples, which allows for an improved understanding of what functional groups may be present at the surfaces of the SOA particles. Furthermore, comparing the particle spectra with those obtained from the gas and condensed phase samples yields information on the molecular environment of the functional groups that may be present on the particle surfaces.

Our previously published work reported that the SFG spectra obtained from fused silica windows in contact with the equilibrium room-temperature vapor pressures of α-pinene, β-pinene, limonene, isoprene, *cis*-2-pentene, *n*-hexene, *n*-pentene, cyclohex-

ene, and cyclopentene did not agree with those obtained from the AMAZE-08 particle samples or the synthetic isoprene-derived SOA particle samples prepared at the HEC (Ebben et al., 2011b). In the context of our current work, Figs. 2 and 3 show that the vibrational SFG spectra of the epoxides and tetraols studied here do not match those obtained from the surfaces of field-derived SOA particles collected during AMAZE-08 either. Figure 2a, however, shows some reasonable agreement between the SFG spectra obtained from the vapor phase/window interface of epoxide 1 and the synthetic SOA particle material/window interface. Most importantly, this compound is the only one whose 2952 cm^{-1} peak position matches that of the synthetic SOA particle material, which occurs at 2955 cm^{-1}, and whose methyl and methylene symmetric C–H stretches at 2880 cm^{-1} and 2850 cm^{-1}, respectively, are also reasonably well matched. An even better match is found for the SFG spectrum of the spin-coated *trans*-β-IEPOX/window interface and the synthetic SOA particle material/window interface. In contrast to the results obtained from epoxide 1, epoxides 2, 3, and 4 at the vapor/window interfaces exhibit SFG peak positions at 2941, 2945, and 2940 cm^{-1}, respectively, and these frequency positions do not agree with those obtained from the synthetic or the natural isoprene-derived SOA material. This result suggests that the surface of spin-coated epoxide 1 is a reasonable representation of the surfaces of the isoprene-derived SOA particles, at least as probed by SFG in the C–H stretching region.

Figure 3 shows that the analogous comparison between the SFG spectra obtained from tetraols 5 and 6 and the synthetic and field-derived SOA particle samples does not result in a reasonable match in the asymmetric C–H stretching region near 2955 cm^{-1} except for perhaps the case of the vapor/window interface of tetraol 6. The symmetric C–H stretching region, however, is not well matched. We conclude that the SFG spectra of the fused silica windows containing the condensed phase, i.e. spin-coated, tetraols do not match those obtained from the synthetic or field-derived SOA material.

4 Spectral fitting and molecular orientation analysis

One benefit of SFG is an exquisite sensitivity to molecular orientation at interfaces. However, the orientation of the oscillators that produce SFG signals may change based on what phase state they are in (Wei et al., 2001). By utilizing the ssp and ppp polarization combinations via the polarization intensity ratio method (Buchbinder et al., 2011; Wang et al., 2005a; Moad and Simpson, 2004), the tilt angle of the C_{3v} symmetry axis and the associated distribution width of the methyl group of *trans*-β-IEPOX (epoxide 1) with respect to the surface normal were predicted. This molecule was chosen because the spectra of this molecule provide the best match to isoprene-derived SOA under both vapor and spin-coated conditions. Briefly, each spectrum was fit with a combination of in-phase and out-of-phase Lorentzian peaks, representing the symmetric and asymmetric C–H stretching vibrational modes of the one methyl and the two methylene groups, as well as Fermi resonances that may be present (see details of the fitting procedures and outcomes in the Supplement). The fits show that the SFG responses are due to the asymmetric and symmetric methyl stretches and a methyl Fermi resonance and not due to the asymmetric and symmetric methylene stretches (or their Fermi resonance).

As shown in the Supplement, spectral fitting yielded a point estimate and standard error for the amplitudes of the methyl symmetric stretch, located near 2880 cm^{-1}, for each polarization combination. Based on the spectral fits to the experimental SFG spectra, we determined a point estimate and standard error, in parentheses, of the ppp/ssp amplitude ratio of 0.31(5). In a separate step, theoretical values of χppp/χssp, where χ is the second order susceptibility of the system under investigation for each of the two polarization combinations, were computed for a range of molecular tilt angles based on the optical properties of the system and assuming monomodal Gaussian distributions ranging from 1 to 40° (at full width half maximum). These theoretical ratios are plotted as a function of tilt angle (Fig. 4). The set of angles for which the theoretical values for each orientation distribution overlap with the experimentally determined values is

then the range of molecular tilt angles of the methyl group with respect to the surface normal. Further information on this method of analysis is provided in the Supplement.

Assuming a 1° distribution, which corresponds to all of the methyl C_{3v} axes being aligned to within 1° of one another, the tilt angle would be 40° from the surface normal (Fig. 5). Including wider orientation distribution functions opens up this cone of tilt angles to a range of 27–52° for vapor phase epoxide, and tilt angles from 0–90° are possible when the Gaussian distribution width is broadened to 40° full width half max (FWHM).

The second radial plot indicates possible tilt angles for the C_{3v} axis of the methyl group in spin-coated epoxide 1. Based on the spectral fits to the experimental SFG spectra, we determined a point estimate and standard error of the ppp/ssp amplitude ratio of 0.39(9). The standard error for this point estimate encompasses all theoretically possible tilt angles, but the point estimate itself results in tilt angles ranging from 53–65°. The tilt angles obtained for the methyl group of epoxide 1 in the condensed phase are comparable, albeit somewhat larger, to those obtained for the vapor/fused silica case. This result indicates that the title angle of the methyl group in *trans*-β-IEPOX (1) depends only weakly on the phase state. We conclude from this result that the phase state which *trans*-β-IEPOX (1) is in might influence the SFG spectra by influencing the orientation distribution of oscillators other than the methyl symmetric stretch. Such an influence of phase state on the SFG spectra is indeed observed for the molecules probed here, including *trans*-β-IEPOX (1). We then conclude that the spectral, as opposed to orientational, analysis discussed in Sect. 3.2.3 suggests that if synthetic isoprene-derived SOA particle material is in fact well represented by *trans*-β-IEPOX (1), its methyl group is likely to be in an environment resembling a condensed phase, rather than a vapor phase.

Based on the radial plots and on observations from the spectral fits of our SFG data, we gain additional insight into the orientation of *trans*-β-IEPOX (1) at the fused silica surface. The absence of symmetric and asymmetric methylene contributions in the spectral fits (vide supra and Supplement) may indicate that the two methylene groups are trans-configured to one another, so that their SFG responses cancel out through destructive interference. The rigid carbon backbone of this molecule, shown in Fig. 5, would allow for the existence of a strong coupling mechanism for the vibrational coherences probed by SFG. Similar long-range coupling and phase interference was recently reported for a nonlinearly active chromophore selectively placed at various positions along a DNA helix (Doughty et al., 2013). It is also possible that the symmetric stretching modes are oriented parallel to the surface, so as not to be probed using the ssp polarization combination, and that the resulting asymmetric stretches of the two methylene groups in *trans*-β-IEPOX (1) are out of phase from one another (Fig. 5).

Based on this discussion, we hypothesize that the epoxide oxygen atom is oriented toward the silica surface, allowing for hydrogen bonding interactions between the epoxide and SiOH groups present on the silica surface. As shown in Fig. 5, this arrangement is consistent with a 40° tilt angle of the methyl group with respect to the surface normal.

Given that the carbon atoms forming the backbone of this molecule are held rigidly in place by the presence of the epoxide ring, only the alcohol groups and their associated methylene groups can rotate freely. We propose that the hydroxyl group located on the carbon atom further away from the methyl group (viz. Figure 5) is rotated toward the surface, so as to reduce steric hindrance between the methylene and the methyl groups. This arrangement would also allow for hydrogen bonding interactions between the SiOH groups and the oxygen from the OH group, in addition to that of the epoxide. If the hydroxyl group on the carbon atom adjacent to the methyl group were to be oriented toward the surface as well, the methylene groups would be trans-configured (consistent with the absence of methylene stretches in the SFG spectra), and H-bonding interactions of the molecule with the surface SiOH groups would be maximized.

A thorough structural and orientational analysis was not carried out for epoxides 2, 3, and 4 or for tetraols 5 and 6. As noted in Sects. 3.2.1 and 3.2.2, we propose that mismatches between the spectra of these compounds and that of isoprene-derived SOA particles may result from a lack of surface activity of these molecules. However,

Discussion Paper | Discussion Paper | Discussion Paper | Discussion Paper |

we cannot rule out that these mismatches may result from differences in orientation of the surface oscillators of these molecules under the phase conditions studied here.

5 Implications for atmospheric chemistry and conclusions

While it is impossible from our study to definitely determine whether the epoxide or tetraol compounds prepared and studied here are part of isoprene-derived SOA particles, our results can be summarized as follows: the SFG spectra obtained from synthetic isoprene-derived SOA particle material are reasonably well reproduced by spin-coated *trans*-β-IEPOX (1) and to a lesser degree by the vapor phase of *trans*-β-IEPOX (1) and also *anti*-2-methyltetraol (6) in contact with a fused silica window. The obvious mismatch of the SFG spectra obtained from the synthetic SOA particle material and the *cis*-β-IEPOX (2), δ-IEPOX (3), α-IEPOX (4), and *syn*-2-methyltetraol (5) samples, in vapor or spin-coated form, indicates that if these species are in fact present in the SOA material, they are not SFG active (SFG signal intensities vanish in centrosymmetric environments under conditions where molecular orientation distributions average to zero) (Boyd, 2003; Shen, 1984). We therefore conclude that *cis*-β-IEPOX (2), δ-IEPOX (3), α-IEPOX (4), and *syn*-2-methyltetraol (5), and possibly *anti*-2-methyltetraol (6), if indeed part of the synthetic SOA material prepared at the HEC or collected during AMAZE-08, are likely to be located in the bulk of the particles and not at their surfaces. Under low relative humidity conditions, for which SOA particle material has been reported to be solid, (Nelson et al., 2001; Huang et al., 2008) these bulk-localized species may therefore not be available for chemical reactions. However, in the absence of a complete orientation analysis of the molecules studied here, we cannot rule out completely that the mismatches between the SFG spectra of the molecules other than *trans*-β-IEPOX and isoprene-derived SOA material are due to changes in molecular orientation.

The compounds discussed in this work will allow us to test the following hypothesis: is SOA particle formation possible, and are the climate-relevant properties of thusly

Discussion Paper | Discussion Paper | Discussion Paper | Discussion Paper |

formed SOA particles impacted when using the first- and second-generation oxidation products described here as opposed to plain terpenes? Compounds 1–6 should have sufficiently high enough vapor pressures for this experiment (Handbook of Chemistry and Physics, 1997). Testing this hypothesis will advance our mechanistic information regarding the formation of SOA particles, specifically during the stages that take the molecular precursors towards the particle phase. This proposed experiment is similar to current chamber studies that begin with one or more terpenes or their derivatives in the presence of one or more oxidants (see, for instance, Prenni et al., 2009; Kiendler-Scharr et al., 2009) followed by chemical and property analysis of the particle phase formed in the chamber, but will vastly increase the chemical diversity and O/C ratios of the molecular precursors through the power of synthetic organic chemistry. Such experiments will allow us to test whether SOA particle formation that began with a given terpene precursor involves one type of molecular species or if multiple species act in concert. The rates of the two pathways just described differ by their order, which can be quantified and be of high value to modeling efforts aimed at understanding and predicting SOA particle formation (Riipinen et al., 2011). Access to the synthetic compounds described here will thus enable us to “fast-forward” through SOA particle formation chemistry and to quantify the relationship between the climate-properties of the SOA particles formed from molecular precursors with varying O/C ratio.

Supplementary material related to this article is available online at http://www.atmos-chem-phys-discuss.net/13/29811/2013/acpd-13-29811-2013-supplement.pdf.

Acknowledgements. CJE gratefully acknowledges support from an NSF Graduate Research Fellowship and MAU gratefully acknowledges support from a NASA Earth and Space Fellowship. This work was supported by the Initiative for Sustainability and Energy at Northwestern (ISEN) and the National Science Foundation (NSF) Environmental Chemical Sciences Program in the Division of Chemistry under Grant No. 1212692. We thank Matthew Rycenga for

assistance with collecting Raman spectra, and Scot T. Martin of Harvard University for helpful discussions.

References

Boyd, R. W.: Nonlinear Optics, Academic Press, New York, 2003. 29828

Buchbinder, A. M., Weitz, E., and Geiger, F. M.: Pentane, Hexane, Cyclopentane, Cyclohexane, 1-Hexene, 1-Pentene, cis-2-Pentene, Cyclohexene, and Cyclopentene at Vapor/I±-Alumina and Liquid/I±-Alumina Interfaces Studied by Broadband Sum Frequency Generation, J. Phys. Chem. C, 114, 554–566, 2009. 29816

Buchbinder, A. M., Gibbs-Davis, J. M., Stokes, G. Y., Peterson, M. D., Weitz, E., and Geiger, F. M.: Method for Evaluating Vibrational Mode Assignments in Surface-Bound Cyclic Hydrocarbons Using Sum-Frequency Generation, J. Phys. Chem. C, 115, 18284–18294, 2011. 29825

Buck, M. and Himmelhaus, M.: Vibrational spectroscopy of interfaces by infrared-visible sum frequency generation, J. Vac. Sci. Technol. A, 19, 2717–2736, 2001. 29821, 29823

Chen, C. Y., Even, M. A., Wang, J., and Chen, Z.: Sum frequency generation vibrational Spectroscopy studies on molecular conformation of liquid polymers poly(ethylene glycol) and poly(propylene glycol) at different interfaces, Macromolecules, 35, 9130–9135, 2002. 29820

Chen, Q., Liu, Y., Donahue, N. M., Shilling, J. E., and Martin, S. T.: Particle-Phase Chemistry of Secondary Organic Material: Modeled Compared to Measured O:C and H:C Elemental Ratios Provide Constraints, Environ. Sci. Technol., 45, 4763, doi:10.1021/es104398s, 2011. 29816

Conboy, J. C., Messmer, M. C., and Richmond, G. L.: Dependence of alkyl chain conformation of simple ionic surfactants on head group functionality as studied by vibrational sum-frequency spectroscopy, J. Phys. Chem. B, 101, 6724, doi:10.1021/jp971867v, 1997. 29820

Conboy, J. C., Messmer, M. C., and Richmond, G. L.: Effect of alkyl chain length on the conformation and order of simple ionic surfactants adsorbed at the D2O/CCl4 interface as studied by sum-frequency vibrational spectroscopy, Langmuir, 14, 6722, doi:10.1021/la980132u, 1998. 29820

Diallo, A. O. and Waters, D. N.: Vibrational spectra and structure of cyclopropane-d1, and dicyclopropyl ketone, Spectrochim. Acta, 44A, 1109, doi:10.1016/0584-8539(88)80080-1, 1988. 29821

Docherty, K. S., Wu, W., Kim, Y. B., and Ziemann, P. J.: Contributions of Organic Peroxides to Secondary Aerosol Formed from Reactions of Monoterpenes with O_3, Environ. Sci. Technol., 39, 4049–4059, 2005. 29813

Doughty, B., Rao, Y., Kazer, S. W., Kwok, S. J. J., Turro, N. J., and Eisenthal, K. B.: Probing the relative orientation of molecules bound to DNA through controlled interference using second-harmonic generation, P. Natl. Acad. Sci. USA, 15, 5756–5758, 2013. 29827

Ebben, C. J., Martinez, I. S., Shrestha, M., Buchbinder, A. M., Corrigan, A. L., Guenther, A., Karl, T., Petäjä, T., Song, W. W., Zorn, S. R., Artaxo, P., Kulmala, M., Martin, S. T., Russell, L. M., Williams, J., and Geiger, F. M.: Contrasting organic aerosol particles from boreal and tropical forests during HUMPPA-COPEC-2010 and AMAZE-08 using coherent vibrational spectroscopy, Atmos. Chem. Phys., 11, 10317–10329, doi:10.5194/acp-11-10317-2011, 2011a.

Ebben, C. J., Zorn, S. R., Lee, S.-B., Artaxo, P., Martin, S. T., and Geiger, F. M.: Stereochemical Transfer to Atmospheric Aerosol Particles Accompanying the Oxidation of Biogenic Volatile Organic Compound, Geophys. Res. Lett., 38, L16807, doi:10.1029/2011GL048599, 2011b. 29816, 29817

Ebben, C. J., Shrestha, M., Martinez, I. S., Corrigan, A. L., Frossard, A. A., Song, W. W., Worton, D. R., Petaja, T., Williams, J., Russell, L. M., Kulmala, M., Goldstein, A. H., Artaxo, P., Martin, S. T., Thomson, R. J., and Geiger, F. M.: Organic Constituents on the Surfaces of Aerosol Particles from Southern Finland, Amazonia, and California Studied by Vibrational Sum Frequency Generation, J. Phys. Chem. A, 116, 8271–8290, 2012.

Esenturk, O. and Walker, R. A.: Surface structure at hexadecane and halo-hexadecane liquid/vapor interfaces, J. Phys. Chem. B, 108, 10631–10635, 2004.

Fontana, A., Messina, R., Spinella, A., and Cimino, G.: Simple and versatile synthesis of branched polyols: (+)-2-C-methylerythritol and (+)-2-C-methylthreitol, Tetrahedron Lett., 41, 7559–7562, 2000. 29815

Galbally, I. E., Lawson, S. J., Weeks, I. A., Bentley, S. T., Gillett, R. W., Meyer, M., and Goldstein, A. H.: Volatile organic compounds in marine air at Cape Grim, Australia, Environ. Chem., 4, 178–182, 2007. 29813

Gao, Y., Hall IV, W. A., and Johnston, M. V.: Molecular Composition of Monoterpene Secondary Organic Aerosol at Low Mass Loadings, Environ. Sci. Technol., 44, 7897–7902, 2010. 29813

Goldstein, A. H. and Galbally, I. E.: Feature Article: Known and Unexplored Organic Constituents in the Earth's Atmosphere, Environ. Sci. Technol., 41, 1515–1521, 2007. 29813

Grassian, V. H.: New Directions: Nanodust – A source of metals in the atmospheric environment?, Atmos. Environ., 43, 6119–6119, 2009. 29813

Greenham, N. C., Peng, X., and Alivisatos, A. P.: Charge separation and transport in conjugated-polymer/semiconductor-nanocrystal composites studied by photoluminescence quenching and photoconductivity, Phys. Rev. B, 54, 17628–17637, 1996. 29813

Hallquist, M., Wenger, J. C., Baltensperger, U., Rudich, Y., Simpson, D., Claeys, M., Dommen, J., Donahue, N. M., George, C., Goldstein, A. H., Hamilton, J. F., Herrmann, H., Hoffmann, T., Iinuma, Y., Jang, M., Jenkin, M. E., Jimenez, J. L., Kiendler-Scharr, A., Maenhaut, W., McFiggans, G., Mentel, Th. F., Monod, A., Prévôt, A. S. H., Seinfeld, J. H., Surratt, J. D., Szmigielski, R., and Wildt, J.: The formation, properties and impact of secondary organic aerosol: current and emerging issues, Atmos. Chem. Phys., 9, 5155–5236, doi:10.5194/acp-9-5155-2009, 2009. 29813

Handbook of Chemistry and Physics: A Ready-Reference Book of Chemical and Physical Data, edited by: Lide, D. R., 78th edn., CRC Press, Inc., Boca Raton, FL, 1997. 29817, 29829

Hatch, C. D. and Grassian, V. H.: 10th Anniversary Review: Applications of analytical techniques in laboratory studies of the chemical and climatic impacts of mineral dust aerosol in the Earth's atmosphere, J. Environ. Monitor., 10, 919–934, 2008.

Heaton, K. J., Dreyfus, M. A., Wang, S., and Johnston, M. V.: Oligomers in the early stage of biogenic secondary organic aerosol formation and growth, Environ. Sci. Technol., 41, 6129–6136, 2007.

Heaton, K. J., Sleighter, R. L., Hatcher, P. G., Hall IV, W. A., and Johnston, M. V.: Composition Domains in Monoterpene Secondary Organic Aerosol, Environ. Sci. Technol., 43, 7797–7802, 2009. 29813

Hommel, E. L. and Allen, H. C.: The air-liquid interface of benzene, toluene, m-xylene, and mesitylene: a sum frequency, Raman, and infrared spectroscopic study, Analyst, 128, 750–755, 2003. 29821

Huang, J., Huang, Z., Jin, S., and Lian, T.: Exciton dissociation in CdSe quantum dots by hole transfer to phenothiazine, J. Phys. Chem. C, 112, 19734–19738, 2008. 29818, 29828

Hudson, P. K., Young, M. A., Kleiber, P. D., and Grassian, V. H.: Coupled infrared extinction spectra and size distribution measurements for several non-clay components of mineral dust aerosol (quartz, calcite, and dolomite), Atmos. Environ., 42, 5991–5999, 2008. 29812, 29814

Huynh, W. U., Dittmer, J. J., Teclemariam, N., Milliron, D. J., Alivisatos, A. P., and Barnham, K. W. J.: Charge transport in hybrid nanorod-polymer composite photovoltaic cells, Phys. Rev. B, 67, 115326, doi:10.1103/PhysRevB.67.115326, 2003. 29813

Kanakidou, M., Seinfeld, J. H., Pandis, S. N., Barnes, I., Dentener, F. J., Facchini, M. C., Van Dingenen, R., Ervens, B., Nenes, A., Nielsen, C. J., Swietlicki, E., Putaud, J. P., Balkanski, Y., Fuzzi, S., Horth, J., Moortgat, G. K., Winterhalter, R., Myhre, C. E. L., Tsigaridis, K., Vignati, E., Stephanou, E. G., and Wilson, J.: Organic aerosol and global climate modelling: a review, Atmos. Chem. Phys., 5, 1053–1123, doi:10.5194/acp-5-1053-2005, 2005. 29813

Keeports, D. D. and Eggers, D. F.: Infrared and Raman spectra of cyclopropane-1,1-d2 and cyclopropane-1,1,2,2-d4, Spectrochim. Acta, 40A, 7–31, 1984. 29821

Kiendler-Scharr, A., Zhang, Q., Hohaus, T., Kleist, E., Mensah, A., Mentel, T. F., Spindler, C., Uerlings, R., Tillmann, R., and Wildt, J.: Aerosol Mass Spectrometric Features of Biogenic SOA: Observations from a Plant Chamber and in Rural Atmospheric Environments, Environ. Sci. Technol., 43, 8166–8172, 2009. 29829

Kleiber, P. D., Grassian, V. H., Young, M. A., and Hudson, P. K.: T-matrix studies of aerosol particle shape effects on IR resonance spectral line profiles and comparison with an experiment, J. Geophys. Res.-Atmos., 114, D21209, doi:10.1029/2009JD012710, 2009. 29813

Lewis, N. S., Crabtree, G., Nozik, A. J., Wasielewski, M. R., and Alivisatos, A. P.: Basic Research Needs for Solar Energy Utilization: Report of the Basic Energy Sciences Workshop on Solar Energy Utilization, U.S. Department of Energy Office of Science, 2005. 29814

Lu, R., Gan, W., Wu, B. H., Chen, H., and Wang, H. F.: Vibrational polarization spectroscopy of CH stretching modes of the methylene goup at the vapor/liquid interfaces with sum frequency generation, J. Phys. Chem. B, 108, 7297–7306, 2004. 29820

Lu, R., Gan, W., Wu, B.-H., Zhang, Z., Guo, Y., and Wang, H.-F.: C-H Stretching Vibrations of Methyl, Methylene and Methine Groups at the Vapor/Alcohol (n = 1–8) Interfaces, J. Phys. Chem. B, 109, 14118–14129, 2005. 29821, 29823

Marple, V. A., Rubow, K. L., and Behm, S. M.: A Microorifice Uniform Deposit Impactor (MOUDI): Description, Calibration, and Use, Aerosol Sci. Technol., 14, 434–446, 1991.

Martin, S. T., Andreae, M. O., Althausen, D., Artaxo, P., Baars, H., Borrmann, S., Chen, Q., Farmer, D. K., Guenther, A., Gunthe, S. S., Jimenez, J. L., Karl, T., Longo, K., Manzi, A.,

Müller, T., Pauliquevis, T., Petters, M. D., Prenni, A. J., Pöschl, U., Rizzo, L. V., Schneider, J., Smith, J. N., Swietlicki, E., Tota, J., Wang, J., Wiedensohler, A., and Zorn, S. R.: An overview of the Amazonian Aerosol Characterization Experiment 2008 (AMAZE-08), Atmos. Chem. Phys., 10, 11415–11438, doi:10.5194/acp-10-11415-2010, 2010a. 29814, 29816, 29817

Martin, S. T., Andreae, M. O., Artaxo, P., Baumgardner, D., Chen, G., Goldstein, A. H., Guenther, A., Heald, C. L., Mayol-Bracero, O. L., McMurry, P. H., Pauliquevis, T., Poeschl, U., Prather, K. A., Roberts, G. C., Saleska, S. R., Dias, M. A. S., Spracklen, D. V., Swietlicki, E., and Trebs, I.: An Overview of the Amazonian Aerosol Characterization Experiment 2008 (AMAZE-08), Rev. Geophys., 48, 11415–11438, 2010b. 29812, 29814

Mena-Carrasco, M., Carmichael, G. R., Campbell, J. E., Zimmerman, D., Tang, Y., Adhikary, B., D'allura, A., Molina, L. T., Zavala, M., García, A., Flocke, F., Campos, T., Weinheimer, A. J., Shetter, R., Apel, E., Montzka, D. D., Knapp, D. J., and Zheng, W.: Assessing the regional impacts of Mexico City emissions on air quality and chemistry, Atmos. Chem. Phys., 9, 3731–3743, doi:10.5194/acp-9-3731-2009, 2009. 29813

Messé, L., Perdigon, A., Clarke, S. M., Castro, M. A., and Inaba, A.: Layer-by-layer surface freezing of linear alcohols at the graphite/liquid interface, J. Colloid Interf. Sci., 266, 19–27, 2003.

Miranda, P. B. and Shen, Y. R.: Liquid interfaces: A study by sum-frequency vibrational spectroscopy, J. Phys. Chem. B, 103, 3292–3307, 1999. 29818, 29820

Moad, A. J. and Simpson, G. J.: A unified treatment of selection rules and symmetry relations for sum-frequency and second harmonic spectroscopies, J. Phys. Chem. B, 108, 3548–3562, 2004. 29825

Murray, C. B., Kagan, C. R., and Bawendi, M. G.: Monodisperse nanocrystals and close-packed nanocrystal assemblies, Annu. Rev. Mater. Sci., 30, 545–610, 2000. 29813

Nelson, J. and Chandler, R. E.: Random walk models of charge transfer and transport in dye sensitized systems, Coordin. Chem. Rev., 248, 1181–1194, 2004. 29814

Nelson, J., Haque, S. A., Klug, D. R., and Durrant, J. R.: Trap-limited recombination in dye-sensitized nanocrystalline metal oxide electrodes, Phys. Rev. B, 63, 205321, doi:10.1103/PhysRevB.63.205321, 2001. 29818, 29828

Opdahl, A., Phillips, R. A., and Somorjai, G. A.: Surface segregation of methyl side branches monitored by sum frequency generation (SFG) vibrational spectroscopy for a series of random poly(ethylene-co-propylene) copolymers, J. Phys. Chem. B, 106, 5212–5220, 2002. 29820

Palaniappan, K., Murphy, J. W., Khanam, N. H., J., Alshareef, H., Quevedo-Lopez, M., Biewer, M. C., Park, S. Y., Kim, M. J., Gnade, B. E., and Stefan, M. C.: Poly(3-hexylthiophene)-CdSe quantum dot bulk heterojunction solar cells: Influence of the functional end-group of the polymer, Macromolecules, 42, 3845–3848, 2009. 29813

Prenni, A. J., Petters, M. D., Faulhaber, A., Carrico, C. M., Ziemann, P. J., Kreidenweis, S. M., and DeMott, P. J.: Heterogeneous ice nucleation measurements of secondary organic aerosol generated from ozonolysis of alkenes, Geophys. Res. Lett., 36, L06808, doi:10.1029/2008GL036957, 2009. 29829

Riipinen, I., Pierce, J. R., Yli-Juuti, T., Nieminen, T., Häkkinen, S., Ehn, M., Junninen, H., Lehtipalo, K., Petäjä, T., Slowik, J., Chang, R., Shantz, N. C., Abbatt, J., Leaitch, W. R., Kerminen, V.-M., Worsnop, D. R., Pandis, S. N., Donahue, N. M., and Kulmala, M.: Organic condensation: a vital link connecting aerosol formation to cloud condensation nuclei (CCN) concentrations, Atmos. Chem. Phys., 11, 3865–3878, doi:10.5194/acp-11-3865-2011, 2011. 29829

Seo, Y.-S. and Satija, S.: No Intrinsic Depletion Layer on a Polystyrene Thin Film at a Water Interface, Langmuir, 22, 7113–7116, 2006.

Sharma, S. N., Pillai, Z. S., and Kamat, P. V.: Photoinduced charge transfer between CdSe quantum dots and p-phenylenediamine, J. Phys. Chem. B, 107, 10088–10093, 2003. 29813

Shen, Y. R.: The Principles of Nonlinear Optics, John Wiley & Sons, New York, 1984. 29828

Spiekermann, M., Bougeard, D., and Schrader, B.: Coupled calculation of vibrational frequencies and intensities II. IR and Raman spectra of cyclopropane, J. Mol. Struct., 60, 55–65, 1980. 29821

Stokes, G. Y., Buchbinder, A. M., Gibbs-Davis, J. M., Scheidt, K. A., and Geiger, F. M.: Heterogeneous Ozone Oxidation Reactions of 1-Pentene, 2-Hexene, Cyclopentene, Cyclohexene, and a Menthenol Derivative Studied by Sum Frequency Generation, J. Phys. Chem. A, 112, 11688–11698, 2008a.

Stokes, G. Y., Buchbinder, A. M., Gibbs-Davis, J. M., Scheidt, K. A., and Geiger, F. M.: Chemically Diverse Environmental Interfaces and Their Reactions with Ozone Studied by Vibrational Sum Frequency Generation, Vib. Spectrosc., 50, 86–98, 2008b.

Stokes, G. Y., Buchbinder, A. M., Gibbs-Davis, J. M., Scheidt, K. A., and Geiger, F. M.: Chemically diverse environmental interfaces and their reactions with ozone studied by sum frequency generation, Vib. Spectrosc., 50, 86–98, 2009a. 29816

Stokes, G. Y., Chen, E. H., Buchbinder, A. M., and Geiger, F. M.: Atmospheric Heterogeneous Stereochemistry, J. Am. Chem. Soc., 131, 13733–13737, 2009b.

Stokes, G. Y., Chen, E. H., Walter, S. R., and Geiger, F. M.: Two Reactivity Modes in the Heterogeneous Cyclohexene Ozonolysis under Tropospherically Relevant Ozone-Rich and Ozone-Limited Conditions, J. Phys. Chem. A, 113, 8985–8993, 2009c. 29816

Sun, B., Marx, E., and Greenham, N. C.: Photovoltaic devices using blends of branched CdSe nanoparticles and conjugated polymers, Nano Letters, 3, 961–963, 2003. 29812, 29814

Tolocka, M. P., Jang, M., Ginter, J. M., Xoc, F. J., Kamens, R. M., and Johnston, M. V.: Formation of oligomers in secondary organic aerosol, Environ. Sci. Technol., 38, 1428–1434, 2004. 29813

Voges, A. B., Al-Abadleh, H. A., and Geiger, F. M.: Applications of Non-Linear Optical Techniques for Studying Heterogeneous Systems Relevant in the Natural Environment, in: Environmental Catalysis, edited by: Grassian, V., CRC Press, Boca Raton, 83–128, 2005. 29816

Voges, A. B., Stokes, G. Y., Gibbs-Davis, J. M., Lettan, R. B., Bertin, P. A., Pike, R. C., Nguyen, S. T., Scheidt, K. A., and Geiger, F. M.: Insights into Heterogeneous Atmospheric Oxidation Chemistry: Development of a Tailor-Made Synthetic Model for Studying Tropospheric Surface Chemistry, J. Phys. Chem. C, 111, 1567–1578, 2007. 29816

Wang, H. F., Gan, W., Lu, R., Rao, Y., and Wu, B. H.: Quantitative spectral and orientational analysis in surface sum frequency generation vibrational spectroscopy (SFG-VS), Int. Rev. Phys. Chem., 24, 191–256, 2005a. 29825

Wang, Q. Q., Zhang, Z., Blackwell, K., and Carmichael, G. G.: Vigilins bind to promiscuously A-to-I-edited RNAs and are involved in the formation of heterochromatin, Curr. Biol., 15, 384–391, 2005b. 29813

Watson, D. F.: Linker-Assisted Assembly and Interfacial Electron-Transfer Reactivity of Quantum Dot-Substrate Architectures, J. Phys. Chem. Lett., 1, 2299–2309, 2010. 29821

Wei, X., Miranda, P. B., and Shen, Y. R.: Surface vibrational spectroscopic study of surface melting of ice, Phys. Rev. Lett., 86, 1554–1557, 2001. 29825

Wei, X., Miranda, P. B., Zhang, C., and Shen, Y. R.: Sum-frequency spectroscopic studies of ice interfaces, Phys. Rev. B, 66, 085401, doi:10.1103/PhysRevB.66.085401, 2002. 29818

Weiss, E. A., Chiechi, R. C., Kaufman, G. K., Kriebel, J. K., Li, Z., Duati, M., Rampi, M. A., and Whitesides, G. M.: Influence of Defects on the Electrical Characteristics of Mercury-Drop Junctions: Self-Assembled Monolayers of n-Alkanethiolates on Rough and Smooth Silver, J. Am. Chem. Soc., 129, 4336–4349, 2007. 29821

Weiss, E. A., Chiechi, R. C., Geyer, S. M., Porter, V. J., Bell, D. C., Bawendi, M. G., and Whitesides, G. M.: Size-dependent charge collection in junctions containing single-size and multi-size arrays of colloidal CdSe quantum dots, J. Am. Chem. Soc., 130, 74–82, 2008a. 29813

Weiss, E. A., Porter, V. J., Chiechi, R. C., Geyer, S. M., Bell, D. C., Bawendi, M. G., and Whitesides, G. M.: The use of size-selective excitation to study photocurrent through junctions containing single-size and multi-size arrays of colloidal CdSe quantum dots, J. Am. Chem. Soc., 130, 83–92, 2008b. 29813

Williams, J., Crowley, J., Fischer, H., Harder, H., Martinez, M., Petäjä, T., Rinne, J., Bäck, J., Boy, M., Dal Maso, M., Hakala, J., Kajos, M., Keronen, P., Rantala, P., Aalto, J., Aaltonen, H., Paatero, J., Vesala, T., Hakola, H., Levula, J., Pohja, T., Herrmann, F., Auld, J., Mesarchaki, E., Song, W., Yassaa, N., Nölscher, A., Johnson, A. M., Custer, T., Sinha, V., Thieser, J., Pouvesle, N., Taraborrelli, D., Tang, M. J., Bozem, H., Hosaynali-Beygi, Z., Axinte, R., Oswald, R., Novelli, A., Kubistin, D., Hens, K., Javed, U., Trawny, K., Breitenberger, C., Hidalgo, P. J., Ebben, C. J., Geiger, F. M., Corrigan, A. L., Russell, L. M., Ouwersloot, H. G., Vil Williams, J., Crowley, J., Fischer, H., Harder, H., Martinez, M., Petäjä, T., Rinne, J., Bäck, J., Boy, M., Dal Maso, M., Hakala, J., Kajos, M., Keronen, P., Rantala, P., Aalto, J., Aaltonen, H., Paatero, J., Vesala, T., Hakola, H., Levula, J., Pohja, T., Herrmann, F., Auld, J., Mesarchaki, E., Song, W., Yassaa, N., Nölscher, A., Johnson, A. M., Custer, T., Sinha, V., Thieser, J., Pouvesle, N., Taraborrelli, D., Tang, M. J., Bozem, H., Hosaynali-Beygi, Z., Axinte, R., Oswald, R., Novelli, A., Kubistin, D., Hens, K., Javed, U., Trawny, K., Breitenberger, C., Hidalgo, P. J., Ebben, C. J., Geiger, F. M., Corrigan, A. L., Russell, L. M., Ouwersloot, H. G., Vila-Guerau de Arellano, J., Ganzeveld, L., Vogel, A., Beck, M., Bayerle, A., Kampf, C. J., Bertelmann, M., Köllner, F., Hoffmann, T., Valverde, J., González, D., Riekkola, M.-L., Kulmala, M., and Lelieveld, J.: The summertime Boreal forest field measurement intensive (HUMPPA-COPEC-2010): an overview of meteorological and chemical influences, Atmos. Chem. Phys., 11, 10599–10618, doi:10.5194/acp-11-10599-2011, 2011. 29813

Yang, C. S.-C., Richter, L. J., Stephenson, J. C., and Briggman, K. A.: In situ, vibrationally resosonant sum frequency spectroscopy study of self-assembly of dioctadecyl disulfide on gold, Langmuir, 18, 7549–7556, 2002. 29822

Yasmeen, F., Vermeylen, R., Szmigielski, R., Iinuma, Y., Böge, O., Herrmann, H., Maenhaut, W., and Claeys, M.: Terpenylic acid and related compounds: precursors for dimers in secondary

organic aerosol from the ozonolysis of α- and β-pinene, Atmos. Chem. Phys., 10, 9383–9392, doi:10.5194/acp-10-9383-2010, 2010. 29812, 29813, 29814

Zhang, Z., Lin, Y.-H., Zhang, H., Surratt, J. D., Ball, L. M., and Gold, A.: Technical Note: Synthesis of isoprene atmospheric oxidation products: isomeric epoxydiols and the rearrangement products *cis*- and *trans*-3-methyl-3,4-dihydroxytetrahydrofuran, Atmos. Chem. Phys., 12, 8529–8535, doi:10.5194/acp-12-8529-2012, 2012. 29815

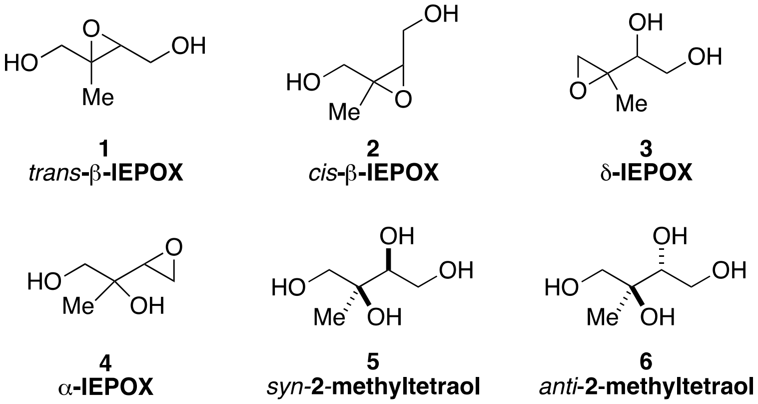

Fig. 1. Chemical structures of the isoprene-derived oxidation products synthesized and analyzed in this work.

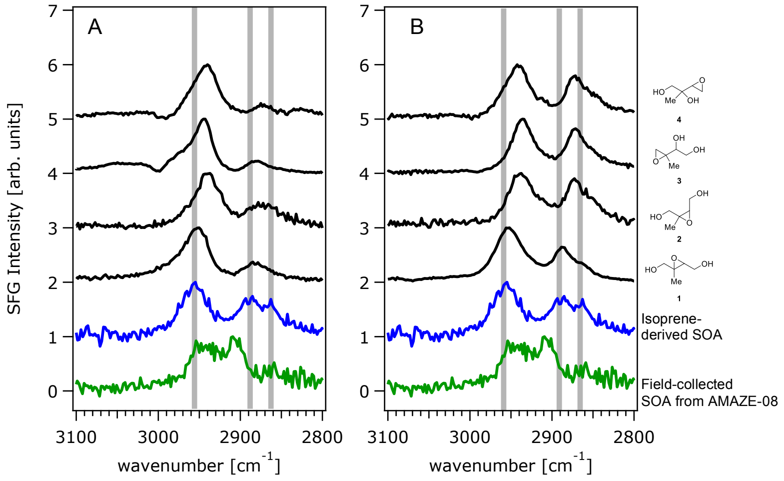

Fig. 2. ssp-Polarized SFG spectra of vapor-phase (left) and spin-coated (right) epoxides in contact with fused silica and comparison to isoprene-derived SOA particles (blue) and SOA particles collected in the central Amazon Basin (green). From top: *α*-IEPOX (4), *δ*-IEPOX (3), cis-*β*-IEPOX (2), trans-*β*-IEPOX (1), isoprene-derived SOA, and natural SOA from the central Amazon Basin. Gray vertical lines indicate (from right) CH_3 asymmetric, CH_3 symmetric, and CH_2 symmetric stretches. Spectra are offset for clarity.

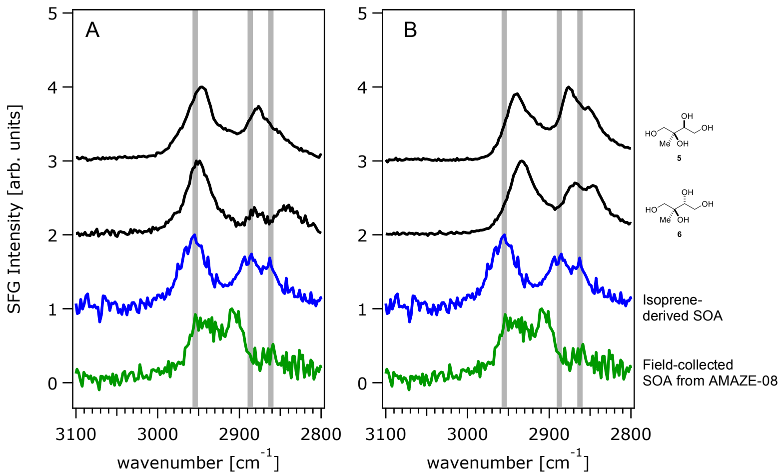

Fig. 3. ssp-Polarized SFG spectra of vapor-phase (left) and spin-coated (right) 2-methyltetraols in contact with fused silica and comparison to isoprene-derived SOA particles (blue) and SOA particles collected in the central Amazon Basin (green). From top: *syn*-2-methyltetraol (5), *anti*-2-methyltetraol (6), isoprene-derived SOA, and natural SOA from the central Amazon Basin. Gray vertical lines indicate CH_3 asymmetric, CH_3 symmetric, and CH_2 symmetric stretches. Spectra are offset for clarity.

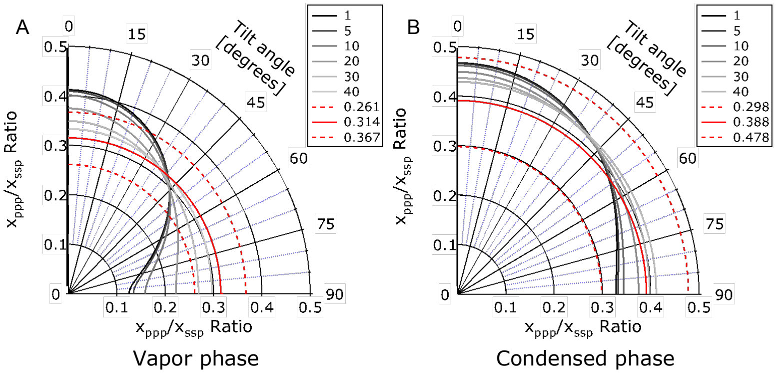

Fig. 4. Radial plots indicating methyl C_{3v} tilt angle as a function of A_{ppp}/A_{ssp} amplitude ratio of the methyl symmetric stretching mode for vapor (left) and spin-coated (right) *trans*-β-IEPOX (1) calculated as described in the text. Solid red curves indicate the experimentally determined ratio point estimates, and dashed red curves indicate the standard errors of these ratios. Gray curves indicate theoretically calculated monomodal Gaussian orientation distributions of widths ranging from 1 to 40°.

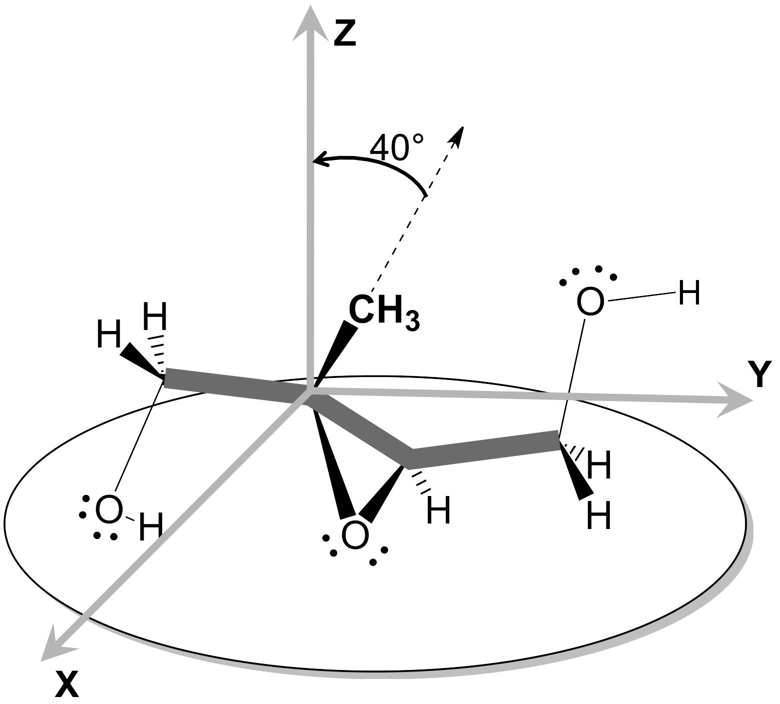

Fig. 5. Proposed model of *trans*-β-IEPOX (1) molecular orientation on a surface. The surface normal is located along the z-axis, with a 40° methyl tilt angle. The rigid backbone of the molecule due to the epoxide ring is indicated by a thick gray line.